Synthesis, Structure, and Magnetic Properties of Bis(3-amino-2-chloropyridinium) tetrahalocuprate (II) [halide= Cl or Br]

Susan N. Herringer,[a] Mark M. Turnbull,[a] Christopher P. Landee,[a] and Jan L. Wikaira[b]

[a] Carlson School of Chemistry and Biochemistry and the Department of Physics, Clark University, 950 Main Street, Worcester, MA 01610 USA

[b] Department of Chemistry, University of Canterbury, Christchurch, New Zealand

Abstract:

The reaction of CuX_2 (X= Cl or Br) with 3-amino-2-chloropyridine in aqueous acids (HX; X= Cl or Br) yields compounds bis(3-amino-2-chloropyridinium) tetrachlorocuprate (II) and bis(3-amino-2-chloropyridinium) tetrabromocuprate (II). Both compounds have been characterized by IR, powder X-ray diffraction, single-crystal X-ray diffraction and temperature dependent magnetic susceptibility. The compounds are isomorphous and exhibit weak antiferromagnetic interactions.

1. Introduction:

Continued interest in low-dimensional magnetic lattices has led to the study of compounds with the general formula $A_2[MX_4]$, where A is an organic cation, M is a 2+ transition metal ion and X is a halide (Cl or Br). The organic cation is usually a protonated base; known compounds have contained bases such as alkyl amines,[1] substituted pyridines,[2] or 2-aminopyrimidine.[3] The Cu(II) ion is an attractive source for the transition metal, M, because of its d^9 configuration and single unpaired electron, making it an S = ½ ion. The absence of a large internal magnetic field, indicated by a g-factor close to 2, allows the Cu (II) ion to follow an external magnetic field.[4] A number of complexes containing the tetrahalocuprate (II) anion have been reported in the literature where the halide is either chloride or bromide.[5, 6, 7] The crystal packing, and hence the distance of the Cu-X····X-Cu non-bonding contacts, is known to affect the magnetic susceptibility of such complexes.[8]

Previously studied is a family of compounds, (2-amino-5-S-pyridinium)$_2$ CuBr$_4$, where S= methyl, Cl, or Br, [5-SAP] whose members are isostructural and exhibit antiferromagnetic interactions.[9, 10] The bulk and the length of the 5-substituent affect the packing motif of the compounds, but also have a significant affect on the exchange interactions within and between the layers.[9] The copper bromide tetrahedra are arranged in square lattices with the organic cations separating them. The 5-substituent on the pyridine ring is positioned within the CuX$_4$$^{2-}$ containing layer, thereby separating the copper halide ions. Within the 5SAP family the order of decreasing magnetic interactions is shown by an increase in the size of the 5-substituent because the magnetic interactions occur through halide···halide contacts.[9] As the size of the substituent decreases, the copper bromide tetrahedra pack more tightly, giving a greater halide···halide overlap and therefore stronger magnetic exchange. The amine group, along with the pyridinium hydrogen, dictate this packing motif by hydrogen bonding to neighboring bromides.[9] As stated above, such changes in crystal packing affect the non-bonding halide-halide contacts and therefore the sign and magnitude of exchange interactions.

Related compounds include (2-amino-3-methylpyridinium)$_2$CuX$_4$ [X = Cl, Br],[11] (3-ammoniumpyridinium)CuX$_4$ [X = Cl, Br],[12] and (2,3-dimethylpyridinium)$_2$CuBr$_4$ which is known to be an antiferromagnetic ladder.[13] The 2-amino-3-methylpyridinium complex, being a 2-aminopyridinium compound, displays typical hydrogen bonding to the CuX$_4$ ions contributing to its tightly packed crystal lattice. (3-Ammoniumpyridinium)CuX$_4$ consists of layers of nearly square planar copper halide ions which are connected to the cations through N-H···X hydrogen bonds. The ammonium group forms three hydrogen bonds, one to a bridging halide and two to

non-bridging halides, while the pyridinium-hydrogen forms bifurcated hydrogen bonds to two halides, one bridging and one nonbridging. These hydrogen bonding patterns cause the halide ions in adjacent layers to pack into nearly opposite relative conformations and halide-halide distances between the layers to be shorter. As mentioned previously, shorter halide-halide contacts produce stronger magnetic exchanges. Bis(2,3-dimethylpyridinium) tetrabromocuprate(II) is a magnetic ladder with significant exchange interactions. Again, the packing is dictated, in part, by the hydrogen bonding with the pyridinium ion, and by its overall size and shape.

The study of magnetic ladders, such as bis(piperidinium)tetrabromocuprate(II)[14] and dibromo-2,3-dimethylpyrazinecopper,[15] has been of much interest in recent years because of the observation linking mechanisms in these systems to those that govern high temperature superconductivity.[16, 17] Given the prior success in generating a magnetic ladder using 2,3-dimethylpyridine and the established use of amino substituents to affect packing, there is interest in creating a family of complexes containing 2,3-disubstituted pyridines, including those with the amino group in the 3-position. The effect of changing the position of the hydrogen bonding amino group on the crystal packing and magnetic susceptibility will be explored. We report here the synthesis, structure and magnetic characterization of bis(3-amino-2-chloropyridinium) tetrachlorocuprate (II) (**1**) and bis(3-amino-2-chloropyridinium) tetrabromocuprate (II) (**2**).

2. Experimental:

2.1 General

2-Amino-3-chloropyridine, hydrochloric acid and hydrobromic acid were purchased from the Aldrich Chemical Company and used without further purification. Copper chloride and copper bromide were obtained from Baker and used without further purification. IR spectra were recorded on a Perkin-Elmer FTIR: Paragon 500.

2.2 Bis(3-amino-2-chloropyridinium) tetrachlorocuprate (II) **(1)**

3-Amino-2-chloropyridine (0.645 g, 5.02 mmol) was dissolved in 2 mL of 6 M HCl (12 mmol). Solid $CuCl_2 \cdot 2H_2O$ (0.426 g, 2.50 mmol) was added to the solution followed by an additional 1mL of 6 M HCl (6 mmol) to ensure complete dissolution. An orange precipitate formed immediately. The mixture was warmed to dissolve the precipitate and the solution was then allowed to cool. Slow evaporation of the dark green aqueous solution at room temperature over the course of eight days gave red crystals of **1** (0.455 g, 39.2%). No attempt was made to maximize the yield. IR (KBr): v 3401w, 3321m, 2853w, 1624s, 1543s, 1465s, 1368m, 1315m, 1134m, 951w, 855w, 792m, 779m, 701cm^{-1}.

2.3 Bis(3-amino-2-chloropyridinium) tetrabromocuprate (II) **(2)**

3-Amino-2-chloropyridine (0.514 g, 4.02 mmol) was dissolved in 3 mL of 4.5N HBr (13.5 mmol). Solid $CuBr_2$ (0.447 g, 2.01 mmol) was added to the solution followed by an additional 2 mL of 4.5N HBr (9 mmol) to ensure complete dissolution. Slow evaporation of the purple aqueous solution at room temperature over the course of twelve days gave dark purple crystals of **2** (0.320 g, 25.0%). IR (KBr): v 3401m, 3305m, 2928m, 2864m, 1624s, 1542s, 1465m, 1366, 1315m, 1136m, 1036w, 941w, 853w, 775m, 699cm^{-1}.

2.4 X-ray structure determination

Data collections were carried out on a Siemens P4 diffractometer employing Mo Kα radiation (λ = 0.71073) and a graphite monochromator. Data collection, cell refinement and data reduction were performed using SHELXTL.[18] Absorption corrections were made via redundant data using SADABS.[19] The structures were solved by direct methods and expanded via Fourier techniques.[20] The non-hydrogen atoms were refined anisotropically. Hydrogen atoms bonded to nitrogen atoms were located in the difference maps and their positions were refined using isotropic U values. The aromatic hydrogen atoms were refined via a riding model with fixed isotropic U values. Full crystal and refinement details are given in Table 1, while selected bond lengths and angles are given in Table 2. Hydrogen bonding parameters are given in Table 3. Crystallographic data were used as the basis of comparison for powder X-Ray diffraction data of the samples used for magnetic studies.

Table 1. Crystal data and structure refinement for **1** and **2**.

	1	**2**
Empirical formula	$C_{10} H_{12} N_4 Cl_6 Cu$	$C_{10} H_{12} N_4 Cl_2 Br_4 Cu$
Formula weight	464.48	642.32
Temperature	262(2)	103(2) K
Wavelength	0.71073 Å	0.71073 Å
Crystal system	Triclinic	Triclinic
Space group	P-1	P-1
Unit cell dimensions		
a (Å)	8.8044(4)	9.1110(5)
b (Å)	9.3047(4)	9.7069(7)
c (Å)	12.5216(5)	12.5707(6)
α (°)	98.940(2)	98.822(4)
β (°)	101.022(2)	100.259(3)
γ (°)	116.664(2)	117.933(2)
Volume (Å³)	865.11(6)	929.98(10)
Z	2	2
Density (calcd) (Mg/m³)	1.783	2.294
Absorption coefficient	2.184 mm^{-1}	10.051 mm^{-1}
F(000)	462	606
Crystal size (mm)	0.40 x 0.30 x 0.04	0.60 x 0.45 x 0.18
Theta range for data collection	1.72 to 31.59°.	1.71 to 31.61°.
Index ranges		
h	$-12 \leq h \leq 12$	$-13 \leq h \leq 12$
k	$-13 \leq k \leq 13$	$-13 \leq k \leq 14$

l	$-18 \leq l \leq 18$	$-17 \leq l \leq 17$
Reflections collected	12457	14683
Independent reflections	5129 [R(int) = 0.0285]	5570 [R(int) = 0.0411]
Completeness to theta = 31.61°	88.3%	88.9 %
Absorption correction	empirical	None
Max./min. transmission	0.9177, 0.4753	0.2649, 0.0650
Refinement method	Full-matrix least-squares on F^2	
Data / restraints / parameters	5129 / 0 / 208	5570 / 0 / 208
Goodness-of-fit on F^2	1.054	1.077
Final R indices [I>2σ(I)]		
R_1	0.0318	0.0332
wR_2	0.0840	0.0755
R indices (all data)		
R1	0.0394	0.0401
$wR2$	0.0918	0.0782
Largest difference peak (e.Å^{-3})	1.091	2.532
Largest difference hole (e.Å^{-3})	-0.775	-1.820

2.5 Magnetic susceptibility

Magnetic data were collected using a Quantum Design MPMS-XL SQUID magnetometer. The

0.0774 g powdered sample of compound **1** and the 0.1104 g powdered sample of compound **2**

used in the magnetic studies were prepared from crushed single crystals. Samples were placed in

gelatin capsules and the magnetic moments were measured using magnetic fields of 0 to 50 kOe

at 1.8 K. Several data points were collected as the magnetic field was brought back to 0 kOe to

confirm that there was no hysteresis. Temperature dependent magnetic susceptibility data was

collected over a temperature range of 1.85-325 K at an applied magnetic field of 1 kOe. The

temperature independent diamagnetic correction of the organic base, 3-amino-2-chloropyridine

was measured to be -30.2 x 10^{-6} emu. Diamagentic corrections for the copper and halide ions

were taken from Pascal's constants.[21] These corrections and the temperature independent

paramagnetic (TIP) correction for the copper atom, 60 x 10^{-6} cm^{3}mol^{-1}, were applied to the data

sets.

3. Results and Discussion:

3.1 Synthesis

The reaction of solid $CuCl_2 \cdot 2H_2O$ with two equivalents of 3-amino-2-chloropyridine and excess

aqueous HCl gave the product bis(3-amino-2-chloropyridinium) tetrachlorocuprate(II) (**1**) in

39.2% yield. Red crystals suitable for X-ray diffraction study crystallized upon slow evaporation

at room temperature over the course of eight days. Similarly, bis(3-amino-2-chloropyridinium)

tetrabromocuprate(II) (**2**), prepared from solid $CuBr_2$, two equivalents of 3-amino-2-

chloropyridine, and excess aqueous HBr, crystallized over the course of twelve days as deep

purple crystals in 25% yield.
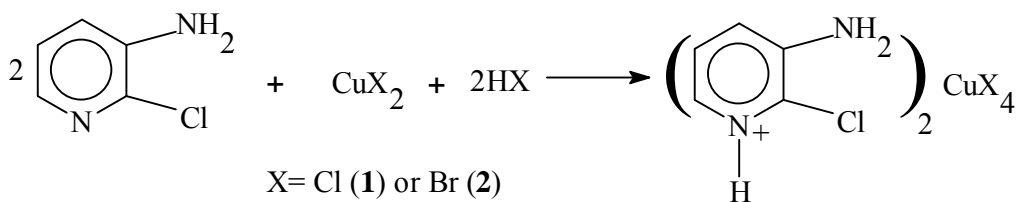
3.2 Analysis of crystal structures

Compounds **1** and **2** both occur as triclinic crystals in the space group P-1. Crystallographic data

for both compounds are given in Table 1. Selected bond lengths and angles are given in Table 2.

Table 3 lists the hydrogen bonding parameters. Both compounds contain distorted CuX_4^{-2} ions.

A common measure of the degree of distortion is to calculate the mean trans angle, or the

average of the two large X-Cu-X angles; idealized tetrahedral and square planar molecules have

bond angles of 109.5° and 180°, respectively.

Table 2.   Bond lengths (Å) and angles (°) for **1** and **2**.

1		**2**	
Bond lengths		*Bond lengths*	
Cu1-Cl1	2.2384(5)	Cu1-Br4	2.3716(5)
Cu1-Cl4	2.2428(5)	Cu1-Br2	2.3739(5)
Cu1-Cl3	2.2651(5)	Cu1-Br3	2.3957(5)
Cu1-Cl2	2.2706(5)	Cu1-Br1	2.4079(5)
N1-C6	1.342(3)	N1-C2	1.338(4)
N1-C2	1.343(2)	N1-C6	1.339(5)
C2-C3	1.397(3)	C2-C3	1.394(5)
C2-Cl5	1.7069(19)	C2-Cl1	1.710(3)
C3-N3	1.344(3)	C3-N3	1.347(5)
C3-C4	1.411(3)	C3-C4	1.407(5)
Bond angles		*Bond angles*	
Cl1-Cu1-Cl4	96.627(19)	Br4-Cu1-Br2	96.085(18)
Cl1-Cu1-Cl3	97.354(19)	Br4-Cu1-Br3	96.773(19)
Cl4-Cu1-Cl3	140.63(2)	Br2-Cu1-Br3	140.26(2)
Cl1-Cu1-Cl2	139.38(2)	Br4-Cu1-Br1	138.94(2)
Cl4-Cu1-Cl2	96.277(18)	Br2-Cu1-Br1	97.368(18)
Cl3-Cu1-Cl2	96.592(19)	Br3-Cu1-Br1	97.153(17)
C6-N1-C2	123.12(19)	C2-N1-C6	123.3(3)
N1-C2-C3	120.76(18)	N1-C2-C3	120.7(3)
N1-C2-Cl5	117.66(15)	N1-C2-Cl1	117.4(3)
C3-C2-Cl5	121.58(14)	C3-C2-Cl1	121.8(3)
N3-C3-C2	121.39(19)	N3-C3-C2	121.1(3)
N3-C3-C4	122.2(2)	N3-C3-C4	122.5(3)
C2-C3-C4	116.43(18)	C2-C3-C4	116.4(3)
C5-C4-C3	120.9(2)	C5-C4-C3	120.8(3)
C4-C5-C6	120.00(19)	C4-C5-C6	120.3(3)
N1-C6-C5	118.79(19)	N1-C6-C5	118.4(3)

3.2.1 X-Ray Structure of bis(3-amino-2-chloropyridinium) tetrachlorocuprate (II) (**1**)

The asymmetric unit of **1** is shown in Figure 1. The $CuCl_4^{-2}$ ions are highly distorted with a mean trans angle of 140°; there is a nearly uniform distortion about the copper with the large Cl-Cu-Cl angles being 139.4° and 140.6°.

The bond lengths and angles for the 3-amino-2-chloropyridinium ions are comparable to that of the related 3-amino-2-chloropyridinium complex -- 3-amino-2-chloropyridinium dihydrogenphosphate.[22] The copper chloride bond lengths are normal, averaging 2.2542(5) Å.

The cations are nearly planar with mean deviations of 0.002 Å and 0.00051 Å from the plane for the N1 and N11 rings, respectively. The amino and chloro substituents are almost co-planar with

the rings, but are bent slightly to opposite sides of the plane. The amino groups (N3 and N13) are rotated $3°$ and $5.3°$ relative to the pyridinium rings. The two cations are canted $63.8°$ to each other.

Molecules of **1** pack in the lattice to generate layers of $CuCl_4^{-2}$ anions parallel to the *ac*-face which are separated by two layers of 3-amino-2-chloropyridinium cations (Figure 2). One layer of cations lies parallel to the face diagonal while the other stacks parallel to the *a*-axis.

Each Cl1 hydrogen bonds to two amino hydrogens ($d_{N3\text{-}H3A\cdots Cl1}$ = 3.305 Å, < 171°; $d_{N3\text{-}H3B\cdots Cl1}$ = 3.324 Å, < 160°), the second of which is an intramolecular hydrogen bond. The pyridinium hydrogens hydrogen bond to Cl2 and Cl3: $d_{N1\text{-}H1\cdots Cl2}$ = 3.1047 Å, < 161°; $d_{N11\text{-}H11\cdots Cl3}$ = 3.1053 Å, < 162°. Only one of the hydrogens in the amino group of the N11 pyridinium hydrogen bonds: $d_{N13\text{-}H13A\cdots Cl4}$ = 3.353 Å, < 162°.

Table 3: Hydrogen bonds for **1** and **2** (Å and °)

D-H...A	d(D-H)	d(H...A)	d(D...A)	<(DHA)
For 1				
N1-H1...Cl2#1	0.84(3)	2.29(3)	3.1047(18)	161(3)
N3-H3A...Cl1#2	0.85(4)	2.46(4)	3.305(2)	171(3)
N3-H3B...Cl1	0.84(4)	2.52(4)	3.324(2)	160(3)
N11-H11...Cl3#3	0.78(3)	2.36(3)	3.1053(18)	162(3)
N13-H13A...Cl4#4	0.85(3)	2.53(3)	3.353(2)	162(3)

Symmetry transformations used to generate equivalent atoms:
#1 x, y+1, z #2 -x, -y+1, -z #3 -x+1, -y+1, -z+1 #4 x-1, y, z

D-H...A	d(D-H)	d(H...A)	d(D...A)	<(DHA)
For 2				
N1-H1...Br1	0.79(5)	2.50(5)	3.244(3)	158(4)
N3-H3A...Br4#1	0.85(6)	2.64(7)	3.424(4)	154(5)
N3-H3B...Br4#2	0.76(6)	2.71(7)	3.432(4)	160(6)
N11-H11...Br3#3	0.84(5)	2.51(5)	3.260(3)	151(4)
N13-H13B...Br2#4	0.82(5)	2.68(5)	3.485(4)	170(5)

Symmetry transformations used to generate equivalent atoms:
#1 x, y-1, z #2 -x-1, -y-1, -z #3 -x, -y, -z+1 #4 x-1, y, z

The $CuCl_4^{-2}$ anions form a linear chain parallel to the *a*-axis (Figure 3). The separation between successive copper halide ions is 4.595 Å, representing the closest Cl···Cl non-bonding contact. The Cu1-Cl1-Cl2A angle is 156.4° and the Cu1A-Cl2A-Cl1 angle is 160.5°. The torsion angle, Cu1-Cl1-Cl2A-Cu1A, between adjacent $CuCl_4^{-2}$ ions is 38.5°. The next closest interaction has a Cl···Cl separation of 4.851 Å.
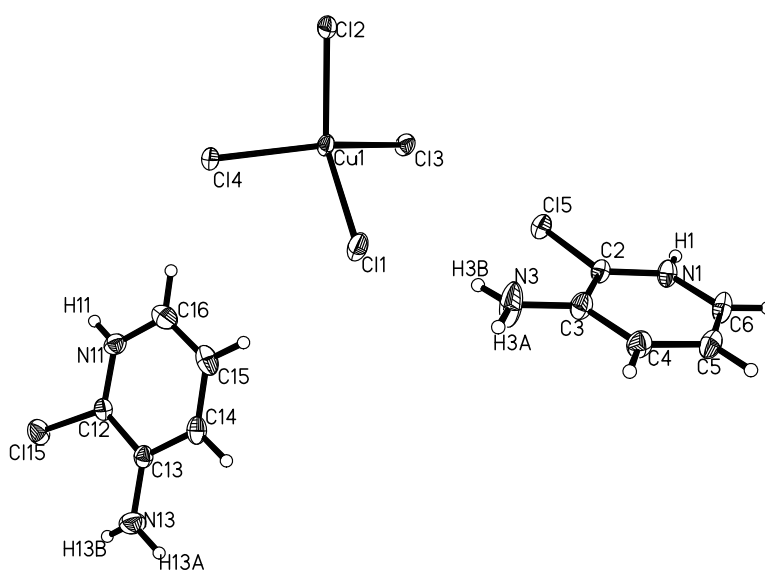
Figure 1: The asymmetric unit of Compound **1** showing 50% probability ellipsoids. Only hydrogen atoms which positions were defined are labeled.
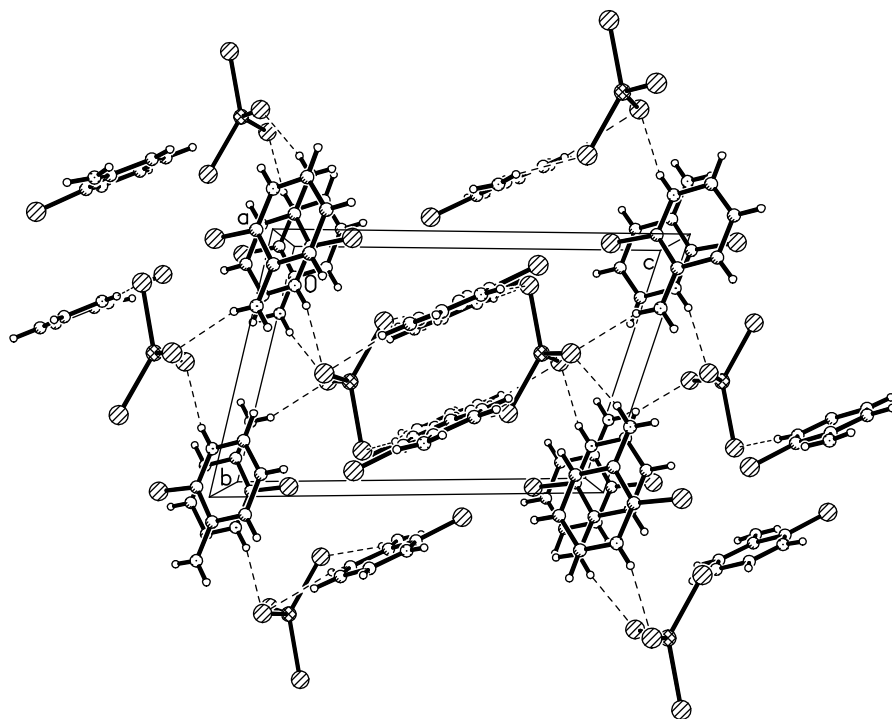
Figure 2: Packing diagram of **1** showing the two orientations of the cations. Dashed lines indicate hydrogen bonds.
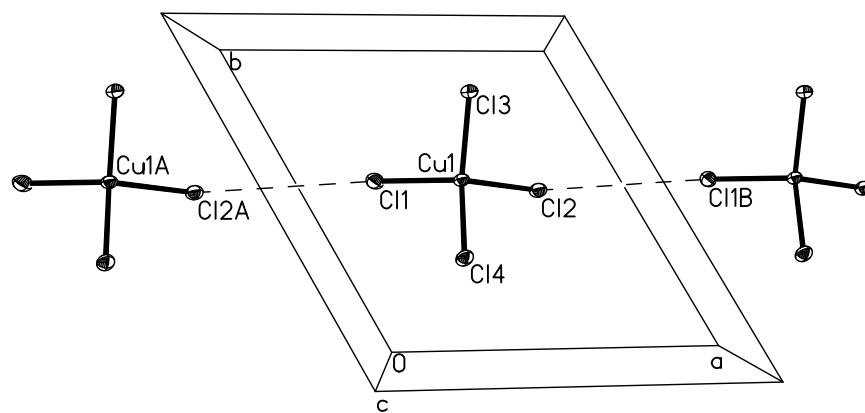
Figure 3: Linear chain of the $CuCl_4^{-2}$ anions. Dashed lines indicate short Cl···Cl contacts.

3.2.2 X-Ray Structure of bis(3-amino-2-chloropyridinium) tetrachlorocuprate (II) (**2**)

Compound **2** also crystallizes in the triclinic space group P-1. The asymmetric unit is shown in

Figure 4. The $CuBr_4^{-2}$ ions are highly distorted with a mean trans angle of 139.6°.

The bond lengths and angles for the 3-amino-2-chloropyridinium cations are comparable to those

in Compound **1** and thus also to those in 3-amino-2-chloropyridinium dihydrogenphosphate.[22]

The copper bromide bond lengths are normal, averaging 2.3873(5) Å, and are slightly longer

than the corresponding Cu-Cl bond lengths as expected. The cations are nearly planar with mean

deviations of 0.0044 Å and 0.0076 Å from the plane for the N1 and N11 rings, respectively.

Similar to Compound **1** the amino and chloro substituents are almost co-planar with the rings,

but are canted toward opposite sides of the plane. The amino groups (N3 and N13) are rotated

11.1° and 8.7° relative to the pyridinium rings. The two cations are canted 60.9° to each other.

Molecules of **2** also pack in the lattice to form layers of $CuBr_4^{-2}$ anions parallel to the *ac*-face

which are separated by two different layers of cations. The packing diagram of **2** is therefore

very similar to **1**, but there is a close contact between the pyridinium chlorine and a bromide

from a CuX_4^{-2} ion (Figure 5). This close contact has been found in many metal-organic salts and

is believed to influence the crystal packing of the salts.[23] The Cl···Br⁻ separation distance, 3.677

Å, is less than the sum of the van der Waals radii of the halogen atom and the ionic radius of the

halide anion. The C-Cl···Br⁻ is nearly linear with an angle of 165.1° which is within the range of

bond angles listed in Awwadi *et al.*[23] The Cu-Br···Cl angle is 101.3° and the torsion angle, Cu1-

Br3···Cl1-C2, is -1.7°.

The hydrogen bonding scheme of **2** is similar to **1** (see Table 3). The pyridinium hydrogens

hydrogen bond to Br1 and Br3: $d_{N1\text{-}H1\cdots Br1}$ = 3.244 Å, < 158°; $d_{N11\text{-}H11\cdots Br3}$ = 3.260 Å, < 151°.

Each Br4 hydrogen bonds to two amino hydrogens: $d_{N3\text{-}H3A\cdots Br4}$ = 3.424 Å, < 154°; $d_{N3\text{-}H3B\cdots Br4}$ =

3.432 Å, < 160°. Only one of the hydrogens in the amino group of the N11 pyridinium hydrogen

bonds: $d_{N13\text{-}H13B\cdots Br2}$ = 3.485 Å, < 170°. As expected, the hydrogen bond lengths of **2** are longer

than those of **1**.

The $CuBr_4^{-2}$ anions form layers parallel to the *b*-face (Figure 6). The closest Br-Br non-bonding

contact distance is 4.652 Å forming a chain of $CuBr_4^{-2}$ ions. The next closest interaction is

formed by Br1-Br4B with a separation distance of 4.682 Å. Together these closest contacts form

a ladder. However, neighboring ladders are not completely isolated; the Br3-Br2C contact has a

separation of 4.912 Å. This distance is within the range of typical separations that are shown to

play a role in magnetic exchange pathways. Bis(2-amino-5-methylpyridinium)

tetrabromocuprate (II), which forms a square lattice, has short contact distances of 4.55 Å and
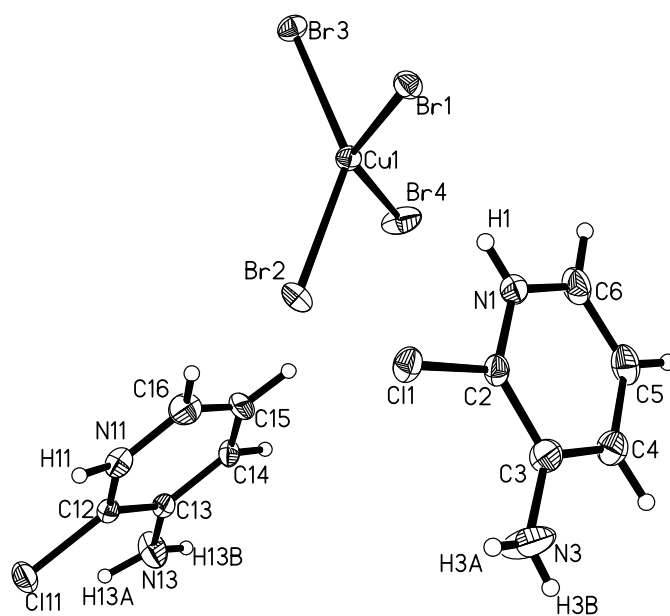
4.97 Å.[24]

Figure 4: The asymmetric unit of Compound **2** showing 50% probability ellipsoids. Only hydrogen atoms which positions were defined are labeled.
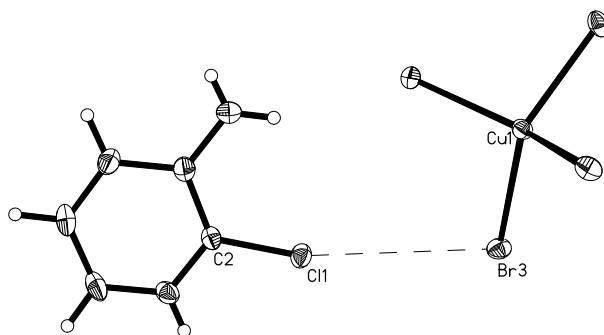

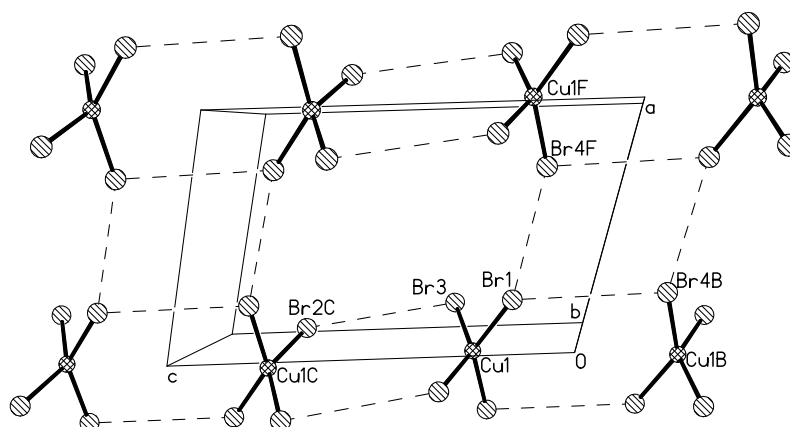Figure 5: Close contact between the pyridinium chlorine and a bromide from a $CuBr_4^{-2}$ ion.

Figure 6: Ladders of the $CuBr_4^{-2}$ anions, which are not completely isolated. Dashed lines represent short Br···Br contacts.

3.3 Magnetic Susceptibility

Magnetic susceptibility data were obtained on powdered samples using a Quantum Design SQUID magnetometer. The molar susceptibility, χ_{mol} ($\chi_{mol} = \lim_{B \to 0} M/B$) was collected as a function of temperature between 1.85 and 325 K for both **1** and **2**. Corrections to molar susceptibility were applied for the temperature-independent magnetization of the Cu (II) ion (60 x 10^{-6} emu mol^{-1}) and the diamagnetic contributions (-157.66 x 10^{-6} and -199.66 x 10^{-6} emu mol^{-1} for the chloride and bromide salts, respectively). Initial corrections made using Pascal's constants (-247.1 x 10^{-6} and -289.1 x 10^{-6} emu mol^{-1} for Compounds **1** and **2**, respectively) gave values for χT which showed a monotonic increase at high temperatures. Therefore, the diamagnetic contributions were recalculated using Pascal's constants for the copper and halide ions, and an experimentally measured value for the organic base (-30.2 x 10^{-6} emu). The diamagnetic correction used for Compound **1** was 63.8% of the initial calculation and that of

Compound **2** is only 69.1% of the initial correction. This change in the diamagnetic correction

resulted in the expected behavior of the χT versus T plot.

The χ^{-1} versus *T* data plots for Compounds **1** and **2** indicate weak antiferromagnetic interactions,

shown by the small negative theta values (**1**: -0.517; **2**: -2.22) extrapolated from the high

temperature portions of the plots. The χT versus T plot (Figure 7) shows that the Curie constant

for **1** is about 0.45 emu*K/mol. The χT versus T plot for **2** (Figure 8) gives a Curie constant of
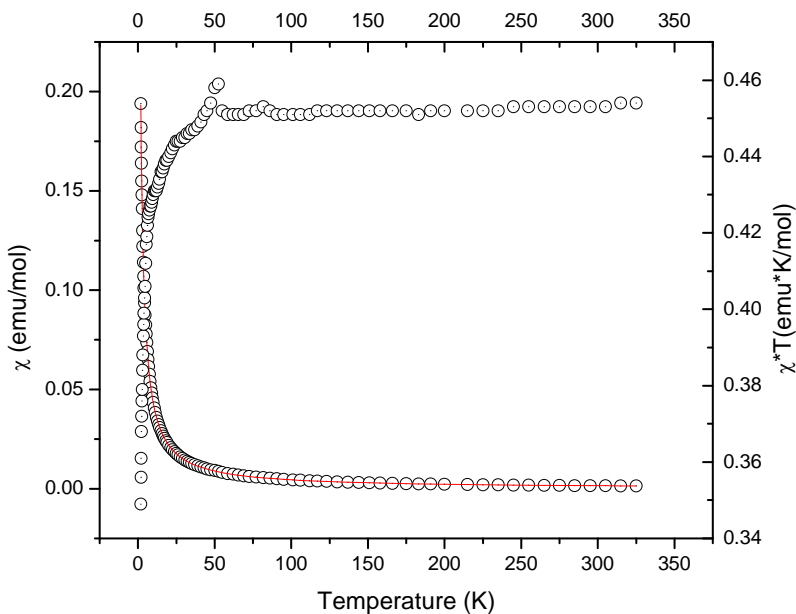
0.41 emu*K/mol.

Figure 7: χ vs. T and χT vs. T plots for **1**. χ vs. T plot is fitted to a liner chain model. The anomaly at 50K in the χT v. T plot is due to trace molecular O_2 in the sample.
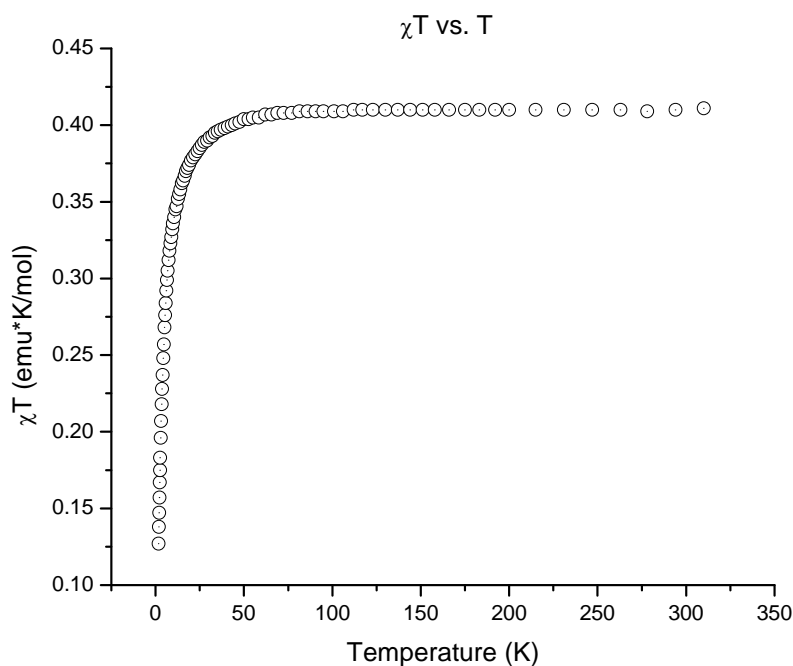
Figure 8: χT vs. T plot for **2**.

The χ versus T plot for **1** (Figure 7) was fit to a linear chain model. Attempts to fit the data to other models including a dimer and two different ladder models gave poor results or unphysical parameters such as negative percent errors. The linear chain model gave 0.448 for the Curie constant and 0.819 for J/k with an R^2 value of 0.99996. This model did result in a paramagnetic impurity of 50%. However, this is an unrealistic value based on powder X-Ray diffraction data, which only indicates a small impurity. By setting the impurity to zero, the model gave comparable values for both the Curie constant and J/k.

The χ versus T plot for **2** (Figure 9) was fit to a two-dimensional antiferromagnetic layer model. Attempts to fit it to a linear chain and two different ladder models gave poor results or unphysical parameters. Table 4 summarizes the Curie constant, J, paramagnetic impurity and R^2

values of the all the models used. Although the two shortest contact distances form a ladder of

$CuBr_4^{-2}$ ions, the close contact between neighboring ladders clearly has a significant role in the

exchange pathway based upon the results of the magnetic data. While the R^2 value for the strong

rail ladder model (0.99996) may statistically represent a good fit, it deviates from the curve at

low temperature. The 2D layer model resulted in the best fit of the curve especially in the low

temperature portion of the curve (see inset of Figure 9). Referring to Table 5, which lists the

short contact distances and angles of the $CuBr_4^{2-}$ anions, the first two contacts are comparable,

but the third is about 9.5% longer than the other two. However, as mentioned previously, this

contact distance is still within the normal range of separation in which exchange pathways are

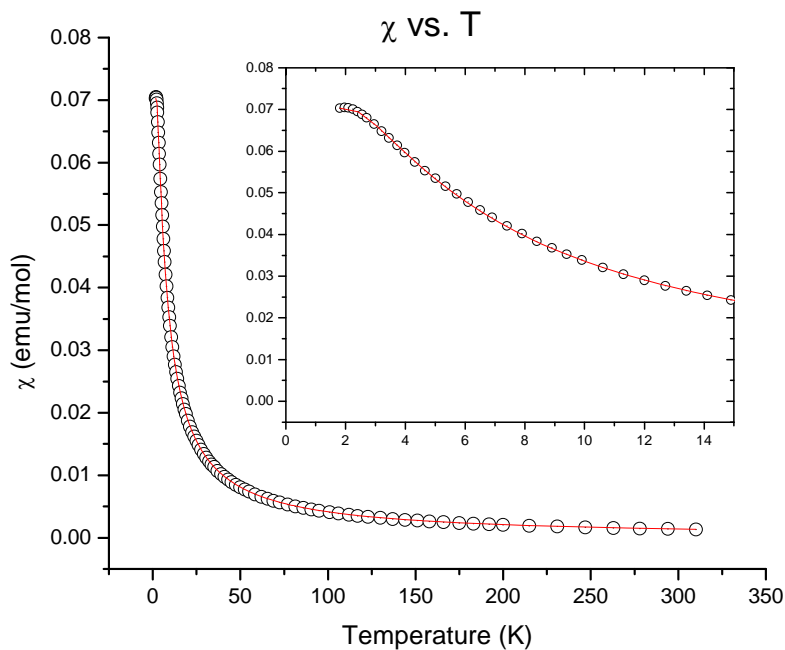seen. Therefore, the magnetic data show that the structure dictates a 2D layer.

Figure 9: χ vs. T plot for **2**. Inset is the expansion of the fit at low temperatures.

Table 4: Data from various models used to fit **2**.

Model	Curie C	J (rail)	J' (rung)	Impurity	R^2
Layer	0.4247	2.47902	--	4.46387	0.99998
Ladder (strong rung)	0.41402	2.94035	2.25128	0.00189	0.9972
Ladder (strong rail)	0.41553	4.00183	2.62427	-6.51875	0.99997
	0.41462	4.12148	2.07526	0	0.99996
Linear Chain	0.41073	3.94506	--	7.12399	0.99992

Table 5: Short contact distances and angles of $CuBr_4^{-2}$ anions (**2**).

	Contact Distance (Å)			Angle (^{o})
Br1···Br4F	4.652	Cu1-Br1-Br4B		126.1
Br1···Br4B	4.682	Cu1B-Br4B-Br1		94.9
Br3···Br2C	4.912	Cu1-Br1-Br4F		160.1
		Cu1F-Br4F-Br1		156.7
		(τ) Cu1-Br1-Br4B-Cu1B		-2.4
		(τ) Cu1-Br1-Br4F-Cu1F		35.4

4. Conclusions:

The bis(3-amino-2-chloropyridinium) tetrachlorocuprate and tetrabromocuprate salts crystallize

in the triclinic space group P-1. Both compounds exhibit weak antiferromagnetic interactions.

The magnetic data for **1** best fits a linear chain model. The magnetic data for **2** best fits the

model of a two dimensional antiferromagnetic layer. Work using other 2,3-disubstitutedpyridine

bases is in progress.

Acknowledgements:

[1] (a) Halvorson, K.; Willett, R.D., Acta Crystallogr., Sect. C 44 2071(1988). (b) Rubenacker, G.V.; Drumheller, J. Magn. Magn. Mater. 79 (1989) 119. (c) Zhou, P.; Drumheller, J.E., J. Appl. Phys. 67 (1990) 5755.

[2] Place, H.; Willett, R.D., Acta Crystallogr., Sect. C 43 (1987) 1050.

[3] (a) Manfredini, T; Pellacani, G.C.; Bonamartini-Corradi, A.; Battaglia, L.P.; Gaurini, G.G.T.; Guisti, J.G.; Willett, R.D.; West, D.X., Inorg. Chem. 29 (1990) 221. (b) Zanchini, C.; Willett, R.D., Inorg. Chem 29 (1990) 3027.

[4] Carlin, Richard L. Magnetochemistry. Springer-Verlag Berlin Heidelberg, Germany; 1986.

[5] Marcotrigiano, G.; Menabue, L.; Pellacani, G. C.. *Journal of Coordination Chemistry*. **1979**, 9, 141-9.

[6] Jeong, Chan-Kyou; Kim, Young-Inn; Choi, Sung-Nak. Bulletin of the Korean Chemical Society (1996), 17(9), 845-849.

[7] Doadrio Lopez, A.; Gutierez Rios, M. T.. Anales de Quimica (1979), 75(3), 228-31.

[8] Snively, L.O.; Tuthill, G.F.; Drumheller, J.E.. Phys. Rev. B 24 (1981) 5349.

[9] Woodward, F.M.; Landee, C.P.; Giantsidis, J.; Turnbull, M.M.; Richardson, C. *Inorganica Chimica Acta.* **2001**, *324*, 324-330 .

[10] Woodward, F.M.; Albrecht, A.S.; Wynn, C.M.; Landee, C.P.; Turnbull, M.M.

[11] Coffey, Thomas J.; Landee, Christopher P.; Robinson, Ward T.; Turnbull, Mark M.; Winn, Mon; Woodward, F.M. *Inorganica Chimica Acta*, **2000**, *303*, 54-60.

[12] Willett, Roger; Place, Helen; Middleton, Michael. *Journal of the American Chemical Society*, **1988**, *26*, 8639-50.

[13] Shapiro, Alexander; Landee, Christopher P.; Turnbull, Mark M.; Jornet, Joaquim; Deumal, Merce; Novoa, Juan J.; Robb, Michael A.; Lewis, William. *Journal of the American Chemical Society*, 2007, 129, 952-959.

[14] Watson, B.C.; Kotov, V.N.; Meisel, M.W.; Hall, D.W.; Granroth, G.E.; Montfrooij, W.T.; Nagler, S.E.; Jensen, D.A.; Backov, R.; Petruska, M.A.; Fanucci, G.E.; Talham, D.R.. *Physical Review Letters.* **2001**, *86*, 5168-5171.

[15] Wells, Brian M.; Landee, Christopher P.; Turnbull, Mark M.; Awwadi, Firas F.; Twamley, Brendan. *Journal of Molecular Catalysis A: Chemical*, **2005**, *228*, 117-123.

[16] Dagotto, E.. *Rep. Prog. Phys*. 1999, 62, 1525.

[17] Sachdev, S. *Science*, 2000, 288, 475.

[18] SHELXTL: v. 5.10, Structure Determination Software Suite, Sheldrick, G.M., Bruker AXS Inc., Madison, WI, 2001.

[19] G.M. Sheldrick. *SADABS. Program for Empirical Absorption Correction of Area Detector Data*, University of Göttingen, Germany, 1996.

[20] G.M. Sheldrick, SHELX97-2. Programs for the Solution and Refinement of Crystal Structures. University of Göttingen, Germany, 1997.

[21] Carlin, Richard L. Magnetochemistry. Germany: Springer-Verlag Berlin Heidelberg. 1986.

[22] Hamed, K.; Samah, A.; Mohamed, R. *Acta Crystallographica, Section E: Struct. Rep. Online*. **2007**, 63, 2896.

[23] Awwadi, Firas F.; Willett, Roger D.; Twamley, Brendan. Crystal Growth & Design **2007**, 7(4), 624-632.

[24] Turnbull, Mark M.; Landee, Christopher P.; Wells, Brian M. *Coordination Chemistry Reviews*, **2005**, 249, 2567-2576.